Protein products of human *Gas2*-related genes on chromosomes 17 and 22 (*hGAR17* and *hGAR22*) associate with both microfilaments and microtubules

Dmitri Goriounov[1], Conrad L. Leung[2] and Ronald K. H. Liem[2,3,*]

[1]Integrated Program in Cellular, Molecular, and Biophysical Studies, [2]Department of Pathology, [3]Department of Anatomy and Cell Biology, Columbia University College of Physicians and Surgeons, New York, NY 10032, USA

*Author for correspondence (e-mail: rkl2@columbia.edu)

Accepted 14 November 2002
Journal of Cell Science 116, 1045-1058 © 2003 The Company of Biologists Ltd
doi:10.1242/jcs.00272

Summary

The human *Gas2*-related gene on chromosome 22 (*hGAR22*) encodes two alternatively spliced mRNA species. The longer mRNA encodes a protein with a deduced molecular mass of 36.3 kDa (GAR22α), whereas the shorter mRNA encodes a larger protein with a deduced molecular mass of 72.6 kDa (GAR22β). We show that both hGAR22 proteins contain a calponin homology actin-binding domain and a Gas2-related microtubule-binding domain. Using rapid amplification of cDNA ends, we have cloned the mouse orthologue of hGAR22, mGAR22, and found its protein products to be extremely well conserved. We also report the cDNA cloning of a human Gas2-related gene on chromosome 17 (hGAR17). *hGAR17* also encodes two protein isoforms. The overall cytoskeletal binding properties of the hGAR17 and hGAR22 proteins are remarkably similar. hGAR17 mRNA expression is limited to skeletal muscle. Although hGAR22 and mGAR22 mRNAs are expressed nearly ubiquitously, mGAR22 protein can only be detected in testis and brain. Furthermore, only the β isoform is present in these tissues. GAR22β expression is induced in a variety of cultured cells by growth arrest. The absolute amounts of GAR22β protein expressed are low. The β isoforms of hGAR17 and hGAR22 appear to be able to crosslink microtubules and microfilaments in transfected cells. This finding suggests that the physiological functions of these proteins may involve integration of these two components of the cytoskeleton.

Key words: Gas2, GAR17, GAR22, Microfilament, Microtubule

Introduction

The cytoskeleton is of crucial importance for both cellular structure and signaling. It is composed of three major components: microfilaments (MFs), microtubules (MTs) and intermediate filaments. Over the past decade, it has become increasingly clear that the individual cytoskeletal subsystems are organized and function in an interdependent manner (Schaerer-Brodbeck and Riezman, 2000; Herrmann and Aebi, 2000; Leung et al., 2002). Proteins have been identified that can link different types of filaments to one another as well as to various kinds of intercellular junctions. Some of the best-studied cytolinker proteins belong to the plakin protein family (Svitkina et al., 1996; Yang et al., 1996; Wiche, 1998; Leung et al., 1999a; Yang et al., 1999).

The human Gas2-related gene on chromosome 22 (hGAR22) was originally identified in a search for putative tumor suppressors (Zucman-Rossi et al., 1996). It is closely related to growth arrest specific gene 2 (Gas2) and is not a member of the plakin family. The primary transcript of *hGAR22* undergoes alternative splicing resulting in two mRNA splice-forms (Zucman-Rossi et al., 1996). The sequences of the hGAR22 proteins contain both a putative calponin homology (CH) actin-binding domain (ABD) and a putative microtubule-binding domain (MTBD) of the recently described Gas2-related (GAR) family (Sun et al., 2001). Nothing is known about the functions or biochemical properties of the protein products of the *hGAR22* gene.

Gas2 was identified in a screen for genes induced in murine fibroblasts by growth arrest (Schneider et al., 1988). Its protein product also contains a CH domain and a GAR domain. Gas2 protein has been shown to associate with MFs in cultured cells, presumably through its CH domain (Brancolini et al., 1992). Its GAR domain colocalizes with MTs in transfected COS7 cells (Sun et al., 2001). Gas2 is phosphorylated on serine and threonine during the G0 to G1 transition. This phosphorylation event is thought to be specifically required for the formation of membrane ruffles following serum stimulation of quiescent cells (Brancolini and Schneider, 1994). Gas2 is cleaved by caspases in cultured cells undergoing apoptosis (Brancolini et al., 1995; Sgorbissa et al., 1999). The resulting N-terminal fragment contains the CH domain and dramatically reorganizes the MF network of the cells, culminating in its collapse around the nucleus. The caspase-mediated cleavage of Gas2 is therefore hypothesized to be necessary for the morphological changes characteristic of apoptotic cells. Consistent with a role of Gas2 in apoptosis, Gas2 expression and cleavage are induced in hindlimb interdigital tissues of mouse embryos between days 13.5 and 15.5, a developmental stage characterized by extensive apoptosis in these tissues (Lee et al., 1999). Whether Gas2 is an indispensable component of the

apoptotic machinery in this or any other in vivo system remains to be determined.

On the basis of the presence of a putative ABD and a putative MTBD in its sequence, hGAR22 could potentially mediate interaction between MFs and MTs in vivo. In this report, we describe the cytoskeleton-binding properties of the hGAR22 proteins as well as their individual domains. We characterize the regulation of GAR22 expression in a number of mammalian cell lines by growth arrest and the GAR22 mRNA and protein expression patterns in both human and mouse tissues. We also report the cDNA cloning of the mouse GAR22 (mGAR22) orthologue and a close human GAR22 homologue, the Gas2-related gene on chromosome 17 (hGAR17).

Materials and Methods

Plasmid construction

All pFLAG-hGAR17 constructs used in this study are schematically depicted in Fig. 1B. pCR2.1-TOPO-hGAR17 clones obtained as a result of hGAR17 cDNA cloning were used as templates in the PCR reactions performed to generate all the pFLAG-hGAR17 plasmids. The construction of the pFLAG vector has been described previously (Leung et al., 1999b). To construct pFLAG-hGAR17α, the PCR product obtained with sense primer 5′-ATGAATTCATCCCAGCCTGCGGGAGGC-3′ and antisense primer 5′-ATTCTAGATTCAGACACTTTGACCATG-3′ was digested with *Eco*RI and *Xba*I and ligated into pFLAG opened with these two enzymes. pFLAG-hGAR17β was similarly constructed using the same sense primer and antisense primer 5′-ATTCTAGATTCAGACCCAGGACTCCTC-3′. To construct pFLAG-hGARD17, sense primer 5′-ATGAATTCACGCAACCTGGACCAGATG-3′ and antisense primer 5′-ATTCTAGATTCATGGCTTGTGTGAGAGGGA-3′ were used. To construct pFLAG-hGARt17 and pFLAG-hCt17, antisense primer 5′-ATTCTAGATTCAGACCCAGGACTCCTC-3′ and sense primers 5-ATTCTAGATTCAGACCCAGGACTCCTC-3′ or 5′-ATGAATTCAGGCAGCTTCCTGAAGCCC-3′ were used, respectively.

All pFLAG-hGAR22 constructs used in this study are schematically depicted in Fig. 1D. The original hGAR22 cDNA clone (GenBank/EMBL/DDBJ accession no. Y07846) was purchased from the I.M.A.G.E. consortium. This clone was used as the template in the PCR reactions performed to generate all the pFLAG-hGAR22 constructs. In order to construct pFLAG-hGAR22α and pFLAG-hGAR22β, the PCR products obtained with sense primer 5′-ATGAATTCAATGGCAGACCCAGTGGCG-3′ and antisense primers 5′-ATTCTAGATTCACCTGGGTGGGGTCTCGGG-3′ and 5′-ATTCTAGATTCACATCCAGGAATCTGG-3′, respectively, were digested with *Eco*RI and *Xba*I and ligated into pFLAG cut at these sites. pFLAG-hCHD22 was similarly constructed using sense primer 5′-ATGAATTCAATGGCAGACCCAGTGGCG-3′ and antisense primer 5′-ATTCTAGATTCACATGCGGGGGCCGCGGGC-3′. For the construction of pFLAG-hGARD22, sense primer 5′-ATGAATTCAACACCCAGCGACCTGCGC-3′ and antisense primer 5′-ATTCTAGATTCACCTGGGTGGGGTCTCGGG-3′ were used. pFLAG-hCt22 was constructed using sense primer 5′-ATGAATTCACCCCGGGATCAGCTGCCC-3′ and antisense primer 5′-ATTCTAGATTCACATCCAGGAATCTGG-3′. pFLAG-hGARt22 was constructed by ligating the PCR product obtained with sense primer 5′-AACACCCAGCGACCTGCGCAAC-3′ and antisense primer 5′-ATTCTAGATTCACATCCAGGAATCTGG-3′ into pFLAG opened at the *Eco*RV and *Xba*I sites. Prior to ligation, the product was digested with *Xba*I and treated with T4 polynucleotide kinase to introduce a phosphate at its 5′ end.

The pET vector system (Novagen) was used to create a prokaryotic expression plasmid used to produce recombinant hGARD22 protein for immunization. pET16b-hGARD22 was constructed by ligating the product of a PCR performed on pFLAG-hGAR22α with sense primer 5′-CTCGACGAGCATATGAGGGAGATTCTG-3′ and antisense primer 5′-CTCGGGATCCTGCATCTCACCTGGGTGG-3′ into pET-16b opened at the *Nde*I and *Bam*HI sites. Prior to ligation, the PCR product was digested with the same two enzymes.

All constructs were sequenced (DNA Sequencing Facility, Columbia University, New York) to ensure the absence of PCR-introduced errors.

cDNA cloning

mGAR22 cDNA was cloned from a mouse brain Marathon-Ready™ cDNA library (Clontech) by 5′ RACE followed by full-length PCR. Two sets of primers, one nested relative to the other, were used sequentially in each 5′ RACE and full-length cDNA amplification. For 5′ RACE, the first set of primers consisted of Adaptor Primer 1 (Clontech) as the sense primer (5′-CCATCCTAATACGACTCACTATAGGGC-3′) and an antisense primer whose sequence (5′-GAACTGTACCAGCCTCGGGGCAAGC-3′) was based on that of a partial mGAR22 EST clone (GenBank/EMBL/DDBJ accession no. AA718230). The second nested set of primers consisted of the sense Adaptor Primer 2 (Clontech; 5′-ACTCACTATAGGGCTCGAGCGGC-3′) and another EST clone-based antisense primer (5′-AGCACCACACTCTTCTCGTTCTTG-3′). Products of the nested 5′ RACE PCR were subcloned into pCR2.1-TOPO (Invitrogen) and sequenced. These sequences were used to design the sense primers used for the amplification of full-length mGAR22 cDNA (5′-CGGGACTTCGTGCAGTGACTCCAC-3′ – first round primer; 5′-TGCAGTGACTCCACTGGCTCTGGGC-3′ – nested primer). The antisense primers were based on a mouse polyA site sequence clone (GenBank/EMBL/DDBJ accession no. M89786; 5′-TATAATGAAGGCTCAGTCCCCAAAA-3′ – first round primer; 5′-AAACAGGAGCTGGAGCAAGACTTTA-3′ – nested primer). Products of the nested full-length PCR were subcloned into pCR2.1-TOPO and sequenced.

Two sets of primers were used to clone full-length hGAR17 cDNA from a human Universal QuickClone™ cDNA library (Clontech) by nested PCR. The first primer set consisted of sense primer 5′-CCACCTCCTGCCCTGCTGGGGTCCA-3′ and antisense primer 5′-CATGGCCATCCTTTTTGCTTCCCTC-3′. The second, nested set consisted of sense primer 5′-GTCCAGCCATGTCCCAGCCTGCGGG-3′ and antisense primer 5′-TTTTGCTTCCCTCCTACCCAACACG-3′. The products of the nested PCR were subcloned into pCR2.1-TOPO and sequenced.

Pfu polymerase (Stratagene) was used in all PCR reactions. Cycling parameters were set according to the library manufacturer's recommendations (Clontech). All sequencing was performed by the Columbia DNA Sequencing Facility (Columbia University, New York).

Antibody production

The C15 antibody was raised against a GAR-domain-containing fragment (AAs 213-337) encoded by pET16b-hGARD22 and containing a histidine tag at its N-terminus. Recombinant protein was produced in BL21 bacteria and purified on Ni^{2+} columns according to the pET system manual (Novagen). Antibodies were raised in rabbits by Pocono Rabbit Farm & Laboratory, Inc. (Canadensis, Pennsylvania). The C15 antibody was affinity purified on Affi-Gel 10 (Bio-Rad) conjugated to recombinant hGARD22 immunogen.

In vitro binding assays

MF and MT-binding assays were performed as described previously (Leung et al., 1999a). The STP3 T7 reticulocyte in vitro transcription/translation system (Novagen) was used to produce

[^{35}S]methionine-labeled hGAR22 and hGAR17 proteins. All proteins were prespun before incubation with MFs or MTs. The Non-Muscle Actin Binding Protein Spin-Down Biochem Kit (Cytsokeleton, Inc.) was used for the MF-binding assays. The Microtubule Associated Protein Spin-Down Assay Kit (Cytoskeleton., Inc.) was used for the MT-binding assays. BioMax X-ray film (Kodak) was used for autoradiography.

Northern blot analyses

Human or mouse Poly A$^+$ RNA Multiple Tissue Northern (MTN^{TM}) blots (Clontech) were hybridized with [^{35}P]dCTP-labeled random-primed species-specific probes corresponding to the +83/+413 region of hGAR22 or mGAR22 or to the +1147/+2385 region of hGAR17β. Hybridization and washing parameters recommended by the manufacturer were used. BioMax X-ray film (Kodak) was used for autoradiography.

Cell culture, transient transfections and fluorescent microscopy

All cells were cultured at 37°C in an atmosphere containing 5% CO_2. COS7 cells were grown in DMEM (Life Technologies, Inc.) supplemented with 10% fetal bovine serum (FBS). CAD cells [a gift from Dona Chikaraishi, Duke University (Qi et al., 1997)] were grown in DMEM-F12 (Life Technologies, Inc.) supplemented with 8% FBS. NIH 3T3 cells were grown in DMEM with 10% calf serum. GC4spc cells [a gift from Peter Burfeind, University of Gottingen, Germany (Tascou et al., 2000)] were grown in DMEM with 10% FBS. In serum starvation experiments, CAD cells were cultured in serum-free DMEM-F12; COS7, NIH 3T3 and GC4 cells were cultured in their appropriate media with the serum content reduced to 0.1%. In nocodazole treatment experiments, cells were treated with 10 μM nocodazole (Sigma) in standard medium for 1.5 hours before being fixed and stained. For transient transfection, cells were seeded on coverslips and transfected with plasmid DNA using LipofectAMINE PLUS reagent (Life Technologies, Inc.). 24 hours after transfection, the cells were fixed with methanol for 5 minutes at –20°C or with 4% paraformaldehyde in PBS for 10 minutes at room temperature, followed by extensive washing in PBS. The cells were then extracted with 0.5% Triton X100 in PBS for 15 minutes at room temperature, blocked with 5% normal goat serum for 30 minutes and incubated with primary antibodies or phalloidin for 1 hour. After washing three times with PBS, the cells were incubated with secondary antibodies for 1 hour, washed with PBS again, and mounted onto slides in Aquamount (Lerner Laboratories). The following reagents were used for cell staining: phalloidin-AlexaFluor-594, phalloidin-AlexaFluor-350 (Molecular Probes), mouse monoclonal anti-FLAG M2 antibody (Sigma), rabbit polyclonal anti-tubulin antibody (Sigma), AlexaFluor-594-conjugated goat-anti-rabbit antibody and AlexaFluor-488-conjugated goat-anti-mouse antibody (Molecular Probes). A Nikon Eclipse 800 fluorescent microscope and a SPOT digital camera were used to capture images of the stained cells. All images were processed using Adobe Photoshop 6.0.

Quantification of triple colocalization

COS7 cells were transiently transfected with pFLAG-hGAR17β, pFLAG-hGAR22β, pFLAG-hGAR17α or pFLAG-hGAR22α and triple-stained for actin, tubulin and the FLAG epitope. 30 cells transfected with each construct were selected randomly and their pictures taken to generate an RGB triple image. A cell was scored as positive if it contained at least one triple-stained (white) filament equal or exceeding one fifth of the length of the cell or at least two triple-stained filaments each equal or exceeding one tenth of the length of the cell. The χ^2 criterion with the Yates discontinuity correction factor was used to compare the observed frequencies of triple colocalization (Bailey, 1981).

Immunohistochemistry

Cryostat sections of paraformaldehyde-fixed testes from 3-week- or 5-month-old C57BL/6 mice were mounted on glass slides, blocked with 5% normal goat serum for 30 minutes at room temperature and incubated with the C15 antibody for 1 hour. The sections were then washed with PBS several times and incubated with TRITC-conjugated goat-anti-rabbit antibody (Sigma) for 1 hour. After extensive washing with PBS, the sections were sealed with coverslips and Aquamount (Lerner Laboratories) and analyzed by fluorescent microscopy.

Immunoprecipitation, western blotting and phosphatase treatment

To prepare cell lysates for immunoprecipitation, cells were washed wish PBS, scraped into 1 ml of lysis buffer (PBS, pH 7.4; 1% Triton X100, protease inhibitors), vortexed briefly, incubated on ice for 10 minutes, and spun at maximum speed in a tabletop centrifuge. The supernatant was collected and rotated at 4°C for 1 hour with 20 μl of the C15 antibody. 40 μl of Sepharose-Protein-A beads (Sigma) was then added and the sample rotated at 4°C for another hour. The beads were washed four times with lysis buffer, boiled in SDS-containing denaturing buffer, and the resulting sample run on an SDS-PAGE gel. The proteins were transferred onto Immobilon^{TM}-P membrane (Millipore), probed with the C15 antibody followed by incubation with HRP-conjugated goat-anti-rabbit antibody. The HRP staining was visualized using the ECL system (Amersham/Pharmacia). Total cell lysates were prepared by boiling cells in denaturing buffer. Mouse tissue extracts were prepared by homogenizing dissected tissues in 50 mM Tris-HCl, pH 6.8, 1% SDS on ice, centrifuging the extract to pellet the debris and boiling the supernatant in denaturing buffer. In phosphatase treatment experiments, GAR22 protein was immunoprecipitated with the C15 antibody from CAD or COS7 cells serum starved for 48 hours, incubated with protein phosphatase 1 or T-cell phosphatase (New England Biolabs) for 30 minutes at 30°C in buffer supplied by the manufacturer and western-blotted and stained as described above.

Results

Molecular cloning of hGAR17 cDNA

A BLASTN search of the GenBank/EMBL/DDBJ database for sequences similar to hGAR22 cDNA resulted in a partial match with a human chromosome 17 genomic clone (GenBank/EMBL/DDBJ accession No. AC006237). Analysis of the clone using the gene prediction program FGENESN 1.1 identified a putative *GAR22*-like gene, which we termed *GAR17*, for *Gas2*-related on chromosome 17. We then used nested PCR to amplify full-length hGAR17 cDNA from a human multiple-tissue cDNA library. We obtained two sequences, apparent products of alternative splicing. The structures of the two hGAR17 cDNA species and their predicted protein products are schematically depicted in Fig. 1A. The shorter transcript, lacking exon 2B, has an open reading frame of 639 bp and encodes a putative protein product of 213 amino acids with a deduced molecular mass of 23.5 kDa. The longer transcript has an open reading frame of 2640 bp and encodes a putative protein of 880 amino acids with a deduced molecular mass of 96.5 kDa. We have designated the two hGAR17 isoforms hGAR17α and hGAR17β, respectively. The first 286 amino acids of hGAR17α and hGAR17β are identical. The last 27 amino acids of hGAR17α are different from the corresponding residues of hGAR17β owing to a frameshift introduced into the hGAR17α transcript by alternative splicing.

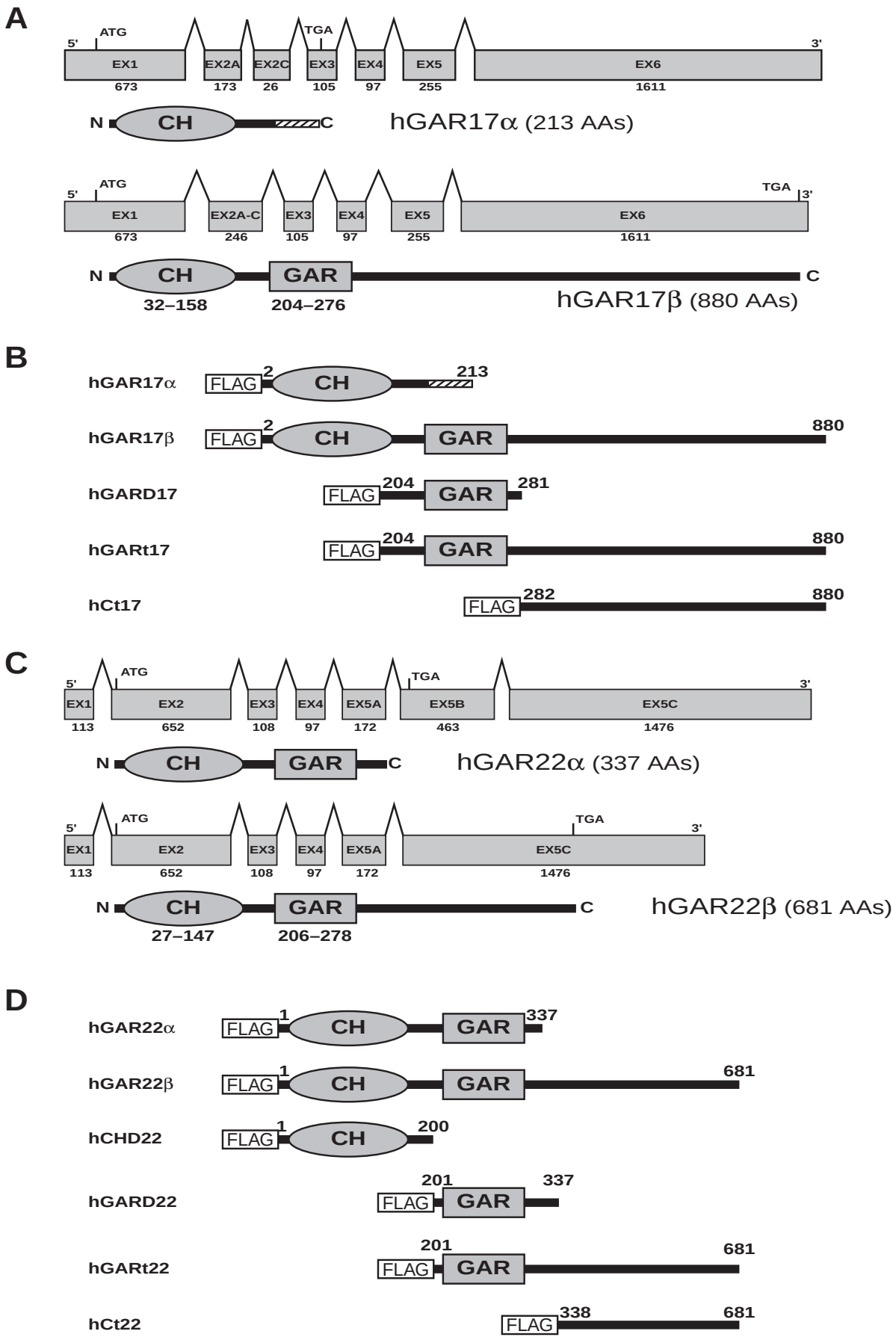
A
5'
ATG
TGA
3'
EX1
EX2A
EX2C
EX3
EX4
EX5
EX6
673
173
26
105
97
255
1611
N
CH
C
hGAR17α (213 AAs)
EX2A-C
246
GAR
32–158
204–276
hGAR17β (880 AAs)
B
hGAR17α
FLAG
2
213
hGAR17β
880
hGARD17
204
281
hGARt17
hCt17
282
C
EX2
EX5A
EX5B
EX5C
113
652
108
172
463
1476
hGAR22α (337 AAs)
hGAR22β (681 AAs)
27–147
206–278
D
hGAR22α
1
337
hGAR22β
681
hCHD22
200
hGARD22
201
hGARt22
hCt22
338

Fig. 1. hGAR17 and hGAR22 isoforms and constructs. (A) hGAR17 mRNA and protein structure. The two mRNA splice forms differ from each other by the presence or absence of exon 2B and encode proteins with deduced molecular masses of 23.5 kDa (isoform α) and 96.5 kDa (isoform β). Exon length in bp is indicated below each exon. hGAR17β contains a calponin homology (CH) domain and a Gas2-related (GAR) domain. The amino acids comprising each domain are indicated. hGAR17α contains only a CH domain. The last 27 amino acids of hGAR17α (hatched box) are different from the corresponding sequence of hGAR17β owing to a frameshift introduced into the α splice form by alternative splicing. The C-terminal sequence of hGAR17β (C-tail 17) does not contain any known domains and is highly degenerate and unstructured.
(B) hGAR17 constructs used in this study. All constructs contain a FLAG epitope tag at their N-terminus. The first and last amino acids of the hGAR17 sequence of each construct are indicated.
(C) hGAR22 mRNA and protein structure. The two mRNA splice forms (see also Zucman-Rossi et al., 1996) differ from each other by the presence or absence of exon 5B and encode proteins with deduced molecular masses of 36.3 kDa (isoform α) and 72.6 kDa (isoform β). Both isoforms contain a calponin homology (CH) domain and a Gas2-related (GAR) domain. The first 337 amino acids of hGAR22β are identical to hGAR22α. The additional C-terminal sequence of hGAR22β (C-tail 22) does not contain any known domains and appears to be highly degenerate and unstructured.
(D) hGAR22 constructs used in this study.

Both hGAR17 isoforms contain a CH domain. hGAR17β also contains a GAR domain and an unstructured C-terminal sequence that we have designated C-tail 17 (Ct17). The N-terminal portions of hGAR17β and hGAR22β display a high degree of sequence similarity. Over the first 337 amino acids, the proteins are ~56% identical, with the CH domains exhibiting ~62% and the GAR domains ~75% sequence identity. The remaining C-terminal sequences are relatively poorly conserved (~30% identity). The hGAR17 sequences are available from GenBank/EMBL/DDBJ under accession Nos. AF508784 (hGAR17α) and AF508785 (hGAR17β).

Cytoskeleton-binding properties of hGAR17 and hGAR22 isoforms

Alternative splicing gives rise to two hGAR22 mRNA splice-forms (Zucman-Rossi et al., 1996) (Fig. 1C). The longer mRNA encodes the hGAR22α protein of 337 amino acids with a deduced molecular mass of 36.3 kDa. The shorter mRNA encodes hGAR22β protein of 681 amino acids with a deduced molecular mass of 72.6 kDa. The first 337 amino acids of hGAR22β are identical to those of hGAR22α and contain a putative ABD of the CH family followed by a putative MTBD of the GAR family. The 334 additional amino acids present at the C-terminus of hGAR22β do not contain any known domains or extended secondary structures. We refer to this portion of hGAR22β as the C-tail 22 (Ct22).

In order to study the cytoskeleton-binding properties of the hGAR17 and hGAR22 isoforms, we subcloned their cDNAs into the eukaryotic expression vector pFLAG, a derivative of pcDNA3 described previously (Leung et al., 1999b) (Fig. 1B,D). The resulting constructs were transiently transfected into NIH 3T3 or COS7 cells. The former cell line showed better stress fibers and was used to study actin colocalization; the latter cell line had a better microtubule network and was used to study MT colocalization. To visualize the transfected proteins (FLAG-tagged at the NH_2 terminus), we used a monoclonal anti-FLAG antibody. Both α isoforms localized predominantly in the cytoplasm, exhibiting strong colocalization with actin filaments, particularly stress fibers (Fig. 2C,F). Neither hGAR17α nor hGAR22α colocalized with MTs, even though the GAR22 protein contains a GAR domain (Fig. 2I,L). Both β isoforms colocalized with actin filaments (Fig. 3C,F). They also showed some colocalization with MTs, which was more evident in some cells than others (Fig. 3I,L). Some of the protein was also distributed in the cytoplasm in a diffuse pattern.

In order to ascertain that the CH and GAR domains of the GAR proteins are functional ABDs and MTBDs, respectively, we created pFLAG constructs encoding amino acids 1-200 of hGAR22 (pFLAG-hCHD22, for CH domain 22), amino acids 201-337 of hGAR22 (pFLAG-hGARD22, for GAR domain 22) or amino acids 204-281of hGAR17β (pFLAG-hGARD17; Fig. 1B,D). The resulting constructs were transfected into NIH 3T3 or COS7 cells and the expressed proteins visualized by antibody staining. hCHD22 protein colocalized with actin filaments (Fig. 4C), suggesting that the CH domain contained within it is likely to be an ABD. Both hGARD17 and hGARD22 proteins exhibited colocalization with MTs, although some of the proteins were also diffusely distributed in the cytoplasm (Fig. 4F,I). These observations indicate that the GAR domains of hGAR17 and hGAR22 are likely to be MTBDs. We also studied the intracellular localization of proteins corresponding to the C-tail portions of hGAR17β (amino acids 282-880, encoded by pFLAG-hCt17) and hGAR22β (amino acids 338-681, encoded by pFLAG-hCt22) as well as of proteins encompassing the GAR domain and the C-tail of the two β isoforms (hGAR17β amino acids 204-880, encoded by pFLAG-hGARt17; hGAR22β amino acids 201-681, encoded by pFLAG-hGARt22; Fig. 1B,D). Both hCt17 and hCt22 proteins colocalized with MTs in a significant fraction of transfected cells; these proteins also tended to accumulate in the nucleus, possibly due to an overall positive charge (Fig. 5C,F). hGARt17 and hGARt22 both colocalized with and apparently bundled MTs in the majority of transfected cells (Fig. 5I,L). These data suggest that the C-tail sequences of the two β isoforms possess an intrinsic MT-binding capacity. This added capacity is probably responsible for the pronounced MT-bundling ability of the GARt fragments. The GARD, Ct and GARt constructs of both hGAR17 and hGAR22 did not exhibit any significant degree of colocalization with MFs in transfected cells. Conversely, hCHD22 did not colocalize with MTs (data not shown).

To assess the MT-stabilizing potential of the various truncated hGAR17 and hGAR22 proteins, we examined their ability to protect MTs from depolymerization by nocodazole in transfected COS7 cells. Consistent with their MT-bundling capacity, only the GARt fragments were able to protect MTs from depolymerization; the preserved MTs also appeared bundled. No other transfected hGAR17 or hGAR22 constructs used in this study conferred on MTs any protection from nocodazole (data not shown).

hGAR17 and hGAR22 proteins bind MFs and MTs in vitro

To verify our findings concerning the cytoskeleton-binding properties of the hGAR17 and hGAR22 proteins in transfected

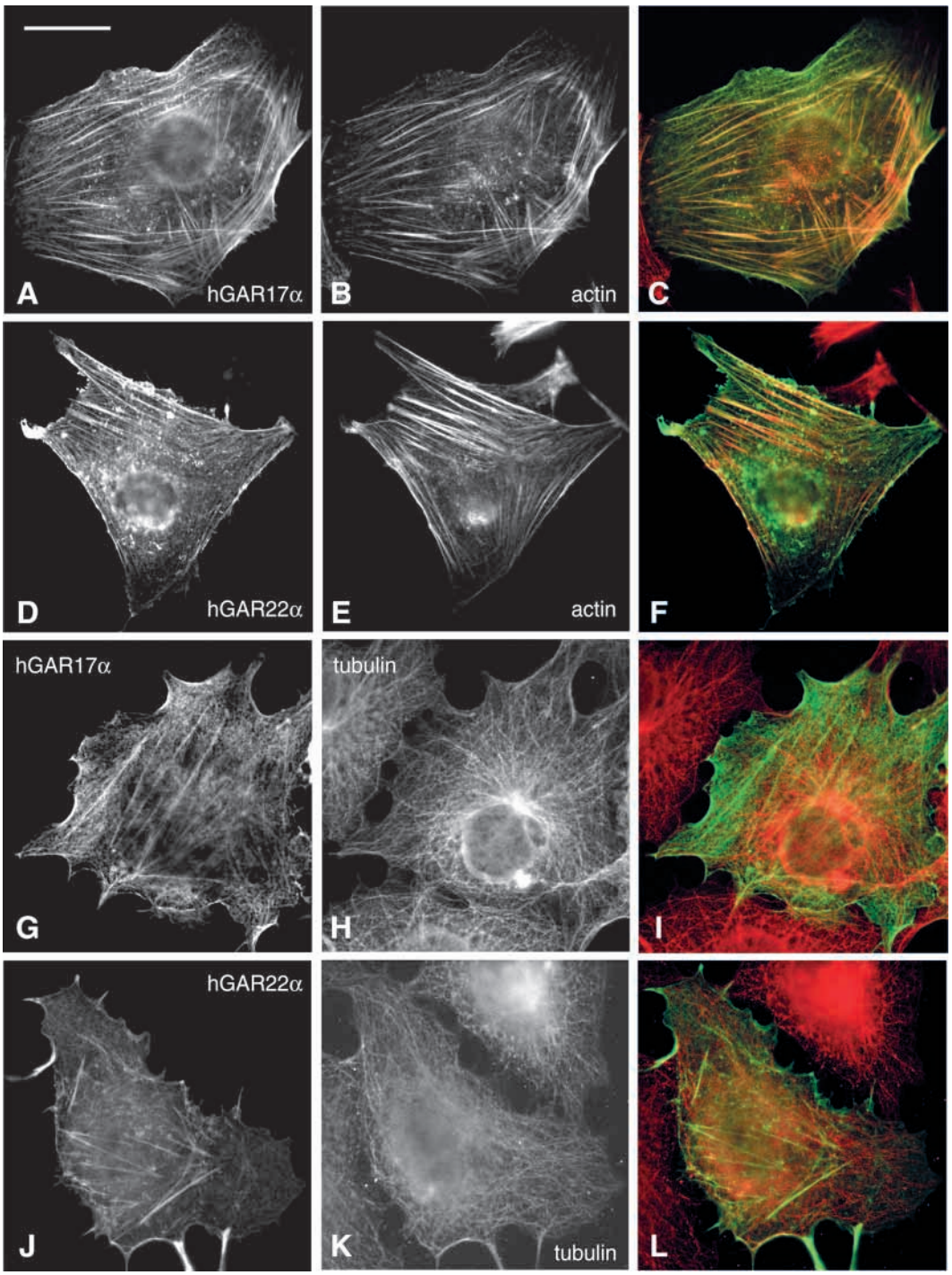

Fig. 2. Localization of the α isoforms of hGAR17 and hGAR22 in transfected cells. NIH 3T3 (A-F) or COS7 (G-L) cells were transiently transfected with pFLAG-hGAR17α A-C; G-I) or pFLAG-hGAR22α (D-F; J-L) and stained with a monoclonal anti-FLAG antibody (A,D,G,J), phalloidin-AlexaFluor-594 (B,E) and a polyclonal anti-tubulin antibody (H,K). (C,F,I,L) Superimposed images, with the FLAG staining in green and the phalloidin or tubulin staining in red. Both α proteins colocalized with MFs (C,F) but not with MTs (I,L). Similar results were obtained with untagged proteins. Bar, 15 μm.

cells, we conducted a series of in vitro binding assays using the same constructs that were used for transient cell transfection. In these assays, radioactively labeled hGAR17 or hGAR22 proteins produced using a reticulocyte lysate in vitro transcription/translation system were incubated with preassembled MFs or MTs, the reactions spun at high speed and the pellet and supernatant fractions run on an SDS-PAGE gel. The labeled proteins were visualized by autoradiography. Any filament-bound protein would be expected to cosediment with the filaments and be present in the pellet fraction, whereas non-bound protein would remain in the supernatant.

As shown in Fig. 6, both hGAR17α and hGAR22α bound MFs in vitro, consistent with their colocalization with actin filaments in transfected cells. Neither α isoform cosedimented with MTs, indicating that the GAR domain of hGAR22α is likely to be masked. The β isoforms bound both MFs and MTs, consistent with their localization in transiently transfected cells. hCHD22 protein cosedimented with MFs but not with MTs. Combined with the finding that hGAR17α binds only MFs in vitro, these data confirm that the CH domains of hGAR17 and hGAR22 are ABDs. hGARD17 and hGARD22 proteins cosedimented only with MTs, indicating that the GAR

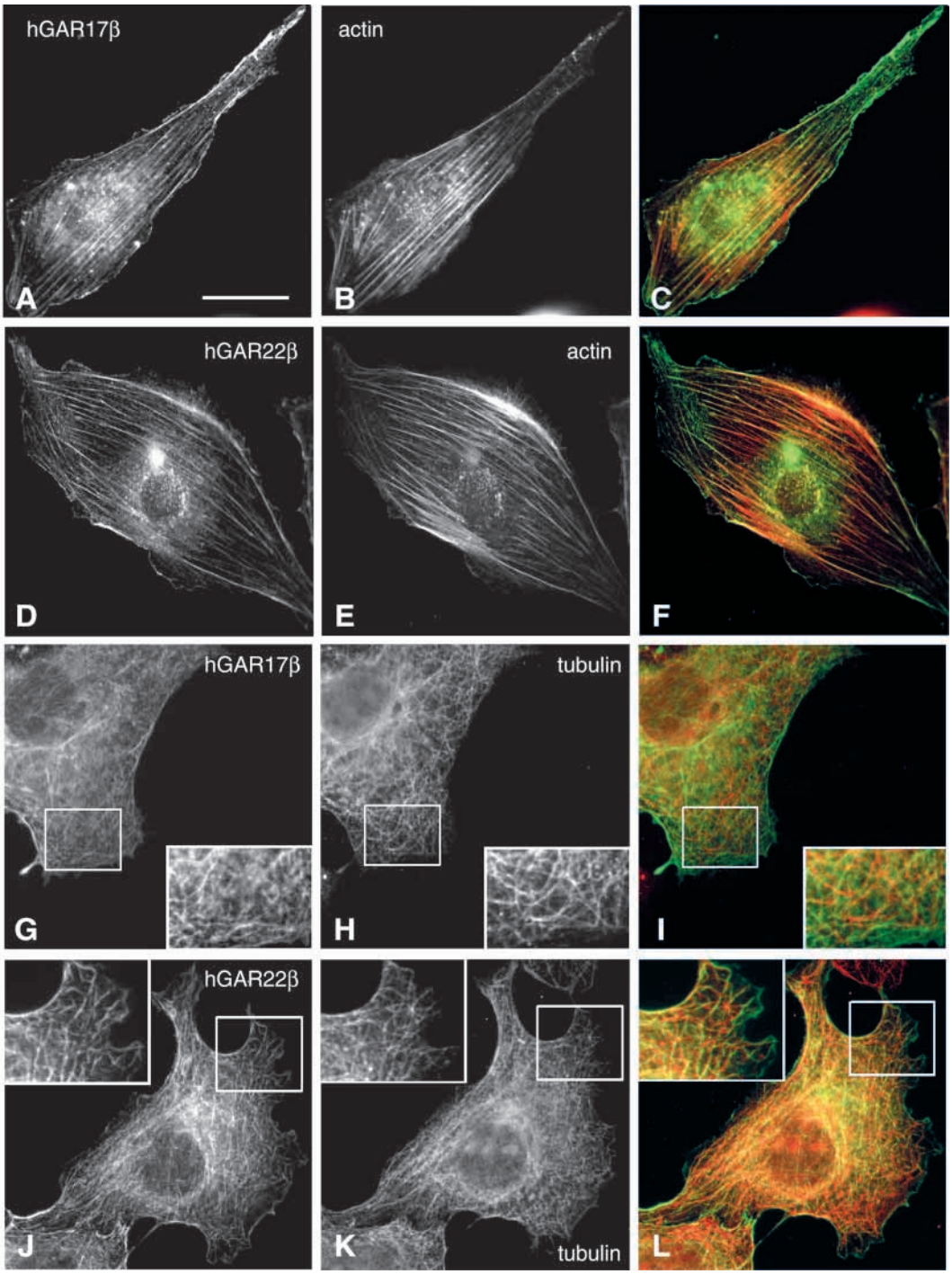

Fig. 3. Localization of the β isoforms of hGAR17 and hGAR22 in transfected cells. NIH 3T3 (A-F) or COS7 (G-L) cells were transiently transfected with pFLAG-hGAR17β (A-C; G-I) or pFLAG-hGAR22β (D-F; J-L) and stained with a monoclonal anti-FLAG antibody (A,D,G,J), phalloidin-AlexaFluor-594 (B,E) and a polyclonal anti-tubulin antibody (H,K). (C,F,I,L) Superimposed images, with the FLAG staining in green and the phalloidin or tubulin staining in red. Both β proteins exhibited colocalization with MFs (C,F) and MTs (I,L; see insets). Bar, 15 μm.

domains of hGAR17 and hGAR22 can bind MTs. Similar results have been shown for the GAR domains of MACF, BPAG1a and Gas 2 (Sun et al., 2001). In addition, like the C-terminal domains of MACF and BPAG1a, the Ct domains of hGAR17β and hGAR22β also bind MTs. Therefore, these two domains may bind cooperatively to MTs.

The cytoskeleton-binding properties and domain organization of the hGAR17 isoforms are remarkably similar to those of the hGAR22 isoforms. The only notable exception is the absence of a GAR domain in hGAR17α. However, the absence of the GAR domain in hGAR17α does not result in cytoskeleton-binding characteristics that are significantly different from those of hGAR22α.

Molecular cloning of mGAR22 cDNA

At present, the mouse is the mammalian model of choice for biomedical researchers, mainly because of its amenability to genetic modification. We therefore were interested in cloning the mouse orthologue of *hGAR22*. To clone mGAR22 cDNA, we used 5′ RACE followed by PCR amplification of full-length cDNA. We obtained two mGAR22 sequences, apparent products

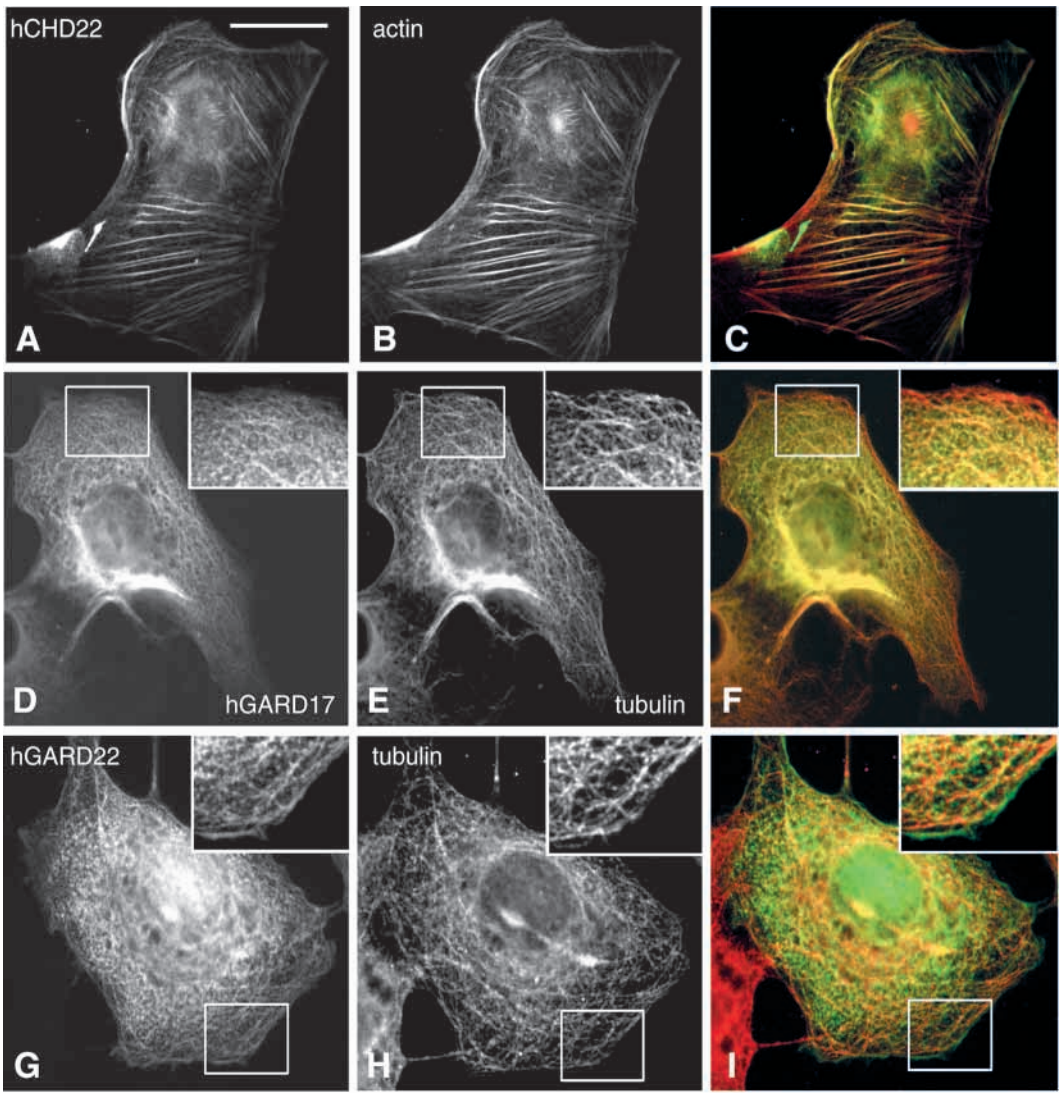

Fig. 4. Localization of the CH and GAR domains in transfected cells. NIH 3T3 (A-C) or COS7 (D-I) cells were transiently transfected with pFLAG-hCHD22 (A-C), pFLAG-hGARD17 (D-F) or pFLAG-hGARD22 (G-I) and stained with a monoclonal anti-FLAG antibody (A,D,G), phalloidin-AlexaFluor-594 (B) and a polyclonal anti-tubulin antibody (E,H). (C,F,I) Superimposed images, with the FLAG staining in green and the phalloidin or tubulin staining in red. hCHD22 protein colocalized with MFs. Both hGARD17 and hGARD22 showed colocalization with MTs (C) (F,I; see insets). Bar, 15 μm.

of alternative splicing. One of them contains an open reading frame of 1011 bp and encodes a putative protein of 337 amino acids with a deduced molecular weight of 36.5 kDa. The sequence of this protein is ~89% identical to that of hGAR22α. This protein represents the mGAR22α isoform. The other amplified cDNA sequence contains an open reading frame of 2034 bp and encodes a putative protein product of 678 amino acids with a deduced molecular mass of 72.4 kDa. This protein is ~87% identical to hGAR22β and represents the mGAR22β isoform. As in the case of hGAR22, the first 337 amino acids of mGAR22β are identical to the sequence of mGAR22α. When transiently expressed in COS7 cells, mGAR22α and mGAR22β exhibited localization patterns practically indistinguishable from those of the corresponding human isoforms (data not shown). The sequences of the mGAR22 cDNAs are available from GenBank/EMBL/DDBJ under accession Nos. AF508323 (mGAR22α) and AF508324 (mGAR22β).

Endogenous expression of GAR17 and GAR22 in tissues and cell lines

Northern blot analysis of human tissues demonstrated that hGAR17 is selectively expressed in skeletal muscle (Fig. 7A). Since hGAR17 α and β splice-form transcripts differ by only 47 bp (Fig. 1A), they cannot be distinguished on a northern blot. However, we have shown by RT-PCR on human muscle mRNA that the β transcript is the predominant hGAR17 mRNA species. In the absence of an anti-GAR17 antibody, we have not yet been able to detect endogenous hGAR17 proteins.

We performed northern blot analyses of GAR22 mRNA expression in both human and mouse tissues. Species-specific probes corresponding to the sequence of GAR22 exon 2 were hybridized with human and mouse multiple-tissue northern blots. In humans, GAR22 mRNA was present in all tissues studied, albeit at greatly varying levels (Fig. 7B). The highest levels of hGAR22 mRNA were detected in the brain, kidney, heart and liver. In all human tissues, the transcripts of hGAR22β (expected size ~2.6 kb) were much more abundant than the transcripts of hGAR22α (~3.1 kb). In mice, the highest levels of GAR22 mRNA were detected in the testes, heart and liver. Substantial amounts were also present in the kidney, brain and lung (Fig. 7C). The shorter transcripts of mGAR22β appeared to be the predominant mGAR22 transcript as well.

To study the expression profiles of GAR22 proteins, we used

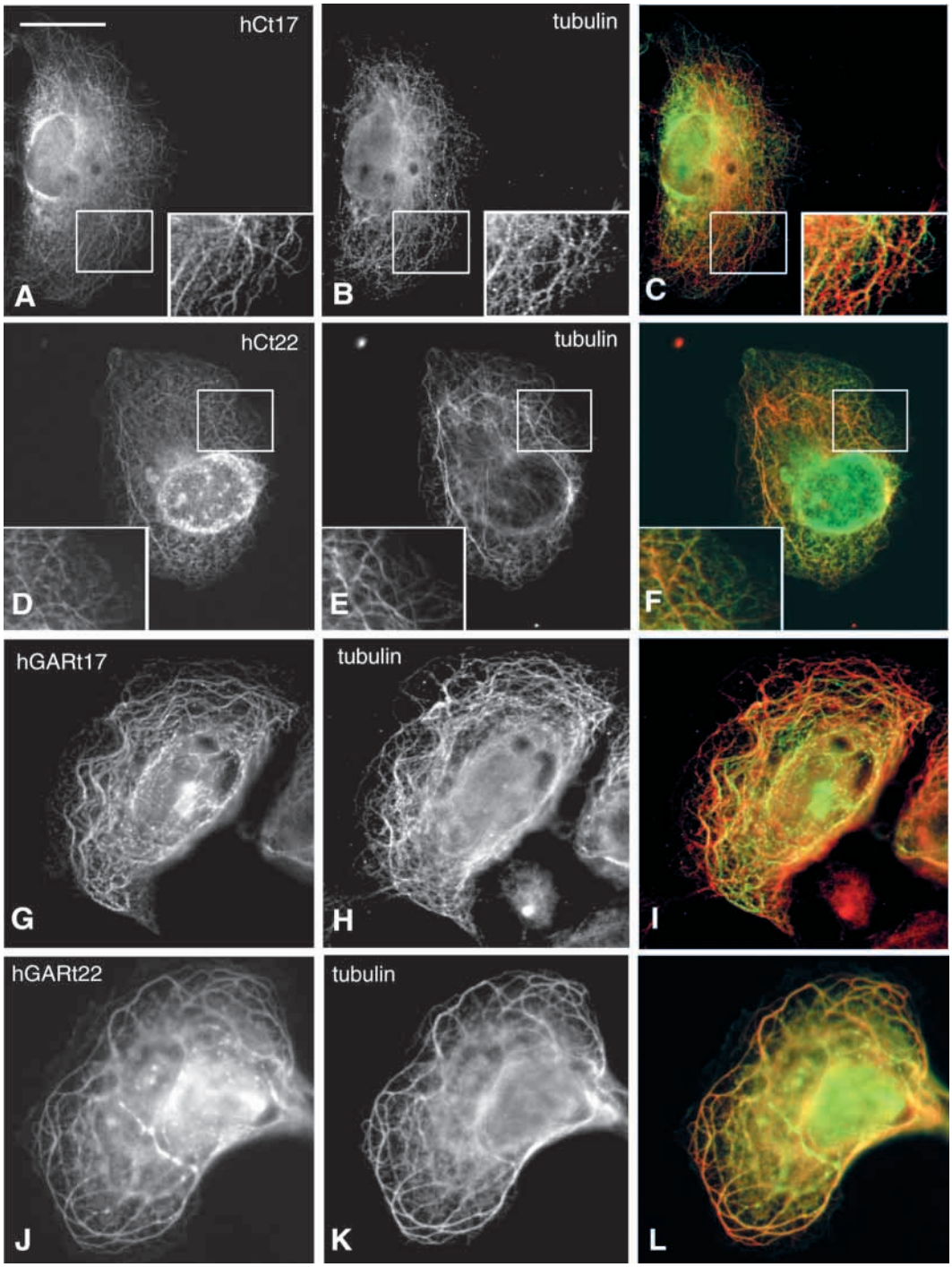

Fig. 5. Localization of C-terminal fragments of hGAR17 and hGAR22 in transfected cells. COS7 cells were transiently transfected with pFLAG-hCt17 (A-C), pFLAG-hCt22 (D-F), pFLAG-hGARt17 (G-I) or pFLAG-hGARt22 (J-L) and stained with a monoclonal anti-FLAG antibody (A,D,G,J) and a polyclonal anti-tubulin antibody (B,E,H,K). Superimposed images, with the FLAG staining in green and the tubulin staining in red, are shown in panels C, F, I and L. Both Ct proteins accumulated in the nucleus (A,D), whereas the cytoplasmic protein showed some colocalization with MTs (C,F; see insets). The GARt fragments colocalized with and appeared to bundle MTs (I,L). Bar, 15 μm.

a rabbit polyclonal antibody, designated C15, that was raised against the hGARD22 region of hGAR22 (Fig. 1D) and affinity purified on recombinant immunogen protein. On western blots of mouse tissues, this antibody recognized a band with an apparent molecular mass of ~75 kDa that comigrated with mGAR22β protein ectopically expressed in COS7 cells. The band was present in testis and, to a lesser degree, in the brain (Fig. 8A). The identity of this band as mGAR22β protein was confirmed by mass spectrometry (data not shown). No bands corresponding to mGAR22α were recognized in any of the tissues studied. Although mGAR22 mRNA was expressed in multiple tissues, the testis and brain appear to be the only mouse tissues that express GAR22β at levels detectable by western blotting. Post-transcriptional inhibition of gene expression or enhanced protein degradation might account for the apparent lack of GAR22 proteins in other GAR22 mRNA-containing tissues. Immunostaining of mouse testicular sections with the C15 antibody showed that mGAR22β is predominantly expressed in the cytoplasm of germ cells at all stages of differentiation. In spermatozoa, the protein was concentrated in the head (Fig. 9).

Gas2, a close homologue of GAR22, has previously been

shown to be upregulated in growth-arrested cultured cells (Brancolini et al., 1992). We therefore studied the effects of growth arrest on GAR22 protein expression in a variety of cultured cell lines of different origin. CAD, NIH 3T3 and GC4 are murine cell lines derived from CNS neurons, fibroblasts and spermatocytes, respectively; COS7 is a simian epithelial cell line. The GAR22 protein was immunoprecipitated from cells that were either actively proliferating or arrested by contact inhibition or serum starvation (CAD cells) for 48 hours, and the precipitated protein detected by western blotting. Both immunoprecipitation and immunodetection were performed with the C15 antibody. In all four cell lines, expression of GAR22β protein was induced by growth arrest (Fig. 8B). No GAR22α was detected in any of the cell lines under any conditions. Growth arrest brought about by serum starvation of the three non-neuronal lines resulted in similar GAR22β induction (data not shown). In CAD cells, GAR22β levels reached a maximum by day 5 of serum starvation (Fig. 8C). In COS7 cells, GAR22β protein levels plateaued by 24 hours of serum starvation (data not shown). As revealed by phosphatase treatment of GAR22β immunoprecipitated from growth-arrested CAD or COS7 cells, the induced protein is likely to be phosphorylated on serine and threonine, but only to a much lesser degree, if at all, on tyrosine (Fig. 8D). In none of the cell lines studied could GAR22 protein be detected by direct western blotting, even in arrested cells. Given that the C15 antibody readily recognizes both GAR22 isoforms in lysates of transfected cells (first lane in Fig. 8A,B and data not shown), this observation suggests that the absolute amounts of endogenous GAR22 protein expressed in cultured cell lines under any conditions are low.

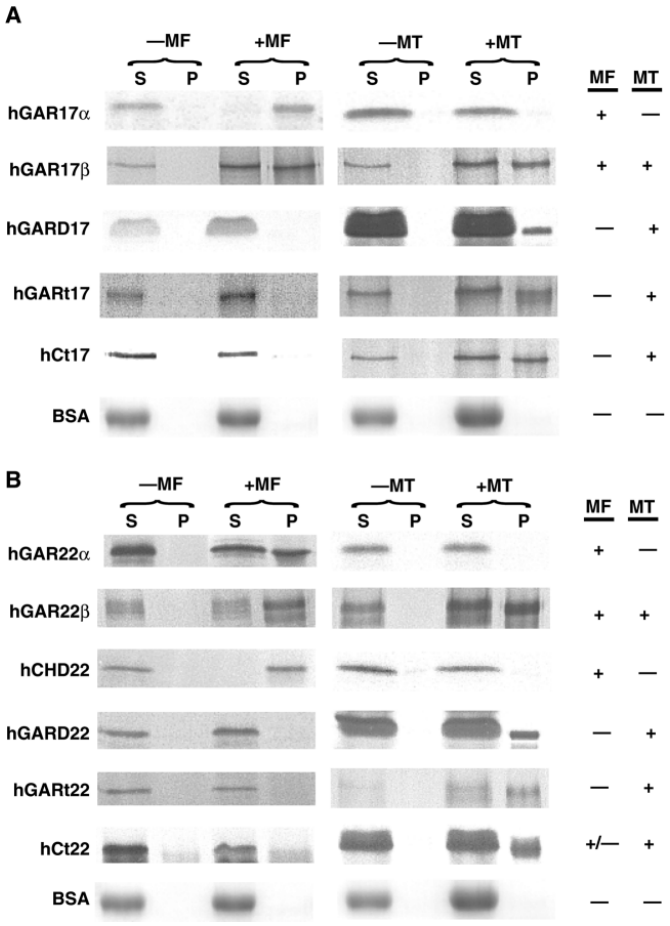

Fig. 6. In vitro binding assays of hGAR17 and hGAR22 proteins. hGAR17 (A) or hGAR22 (B) proteins labeled with ^{35}[S]-methionine were incubated with preassembled MFs (+MF) or MTs (+MT), the reaction mixtures centrifuged at high speed and the resulting supernatant (S) and pellet (P) fractions run on an SDS-PAGE gel. The gels were dried and the radioactively labeled proteins visualized by autoradiography. The presence of a protein in a pellet fraction indicates binding to the corresponding filaments. Reactions without filaments (–MF, –MT) were run to control for non-specific protein aggregation. BSA was used as a non-binding negative control; in this case the protein was visualized by Coomassie staining. The results of the assays are indicated to the right of the gels (+, binding; –, absence of binding). Since hCt22 sedimented in the absence of MFs, its sedimentation with MFs (+/–) is most probably due to non-specific aggregation rather than specific filament binding.

hGAR22β and hGAR17β are likely to crosslink MFs and MTs in transfected cells

hGAR22β and hGAR17β proteins contain both an ABD and an MTBD and can associate with either MFs or MTs in transfected cells (Fig. 3). These findings suggest that these

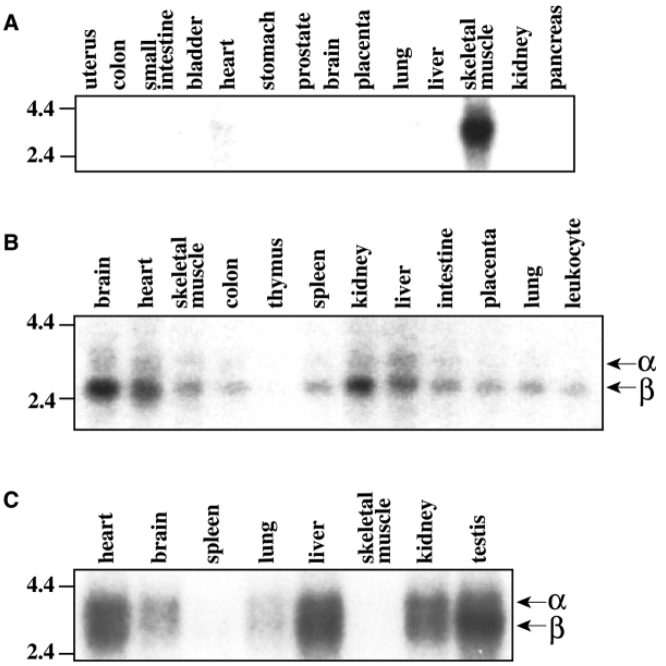

Fig. 7. Expression of GAR17 and GAR22 mRNAs in mammalian tissues. (A) Northern blot analysis of GAR17 expression in human tissues. A human multiple-tissue northern blot was hybridized with a hGAR17-specific probe. As mRNAs of hGAR17α and hGAR17β differ from each other by only 47 bp, they cannot be distinguished on a northern blot. (B) Northern blot analysis of GAR22 expression in human tissues. A human multiple-tissue northern blot was hybridized with a hGAR22-specific probe. hGAR22 α and β transcripts are indicated with arrows. (C) Northern blot analysis of GAR22 expression in mouse tissues. A mouse multiple-tissue northern blot was hybridized with a mGAR22-specific probe. mGAR22 α and β transcripts are indicated with arrows. The sizes of molecular mass markers are in kb.

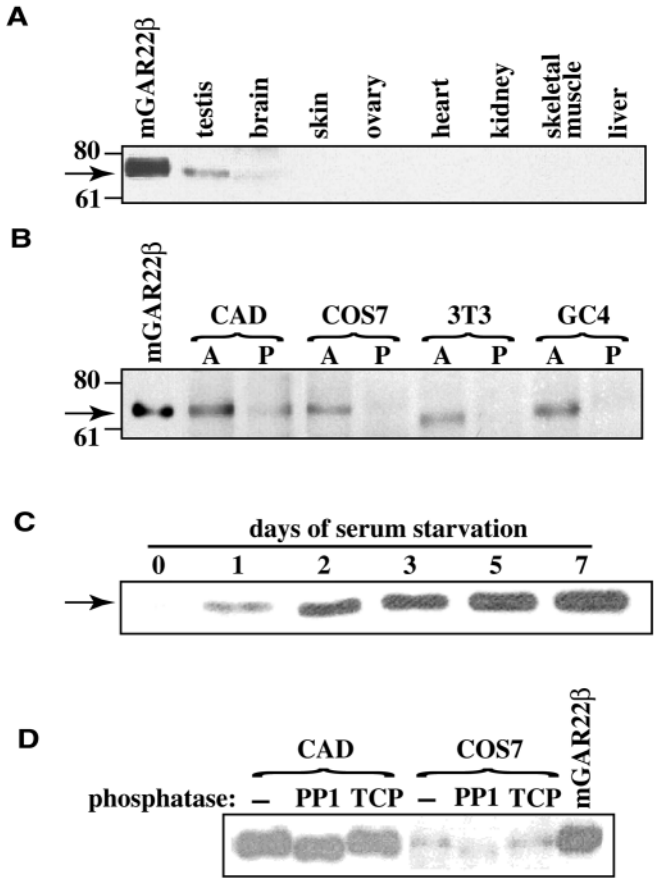

Fig. 8. Expression of GAR22 proteins in mammalian tissues and cells. (A) Western blotting of mouse tissues. Proteins extracts from various mouse tissues were resolved on an SDS-PAGE gel, transferred onto Immobilon membrane, and probed with polyclonal anti-GAR22 C15 antibody. mGAR22β was detected in testis and, at a lower level, in brain (indicated with arrowhead). No mGAR22α protein could be detected in any of the tissues. The sizes of molecular mass markers are in kDa. (B) GAR22 immunoprecipitation from growing or arrested cultured cells. GAR22 protein was precipitated with C15 antibody from either proliferating (P) or growth-arrested (A) cells, run on an SDS-PAGE gel, transferred onto Immobilon membrane and probed with C15 antibody. Expression of GAR22β was induced by growth arrest in all four cell lines. No GAR22α could be precipitated from any of the cell lines. CAD cells were arrested by serum starvation for 48 hours. COS7, NIH 3T3 and GC4 cells were arrested by contact inhibition for 48 hours. (C) Time course of GAR22β induction in growth-arrested CAD cells. GAR22 protein was immunoprecipitated with the C15 antibody from CAD cells serum starved for indicated periods of time. The precipitated protein was visualized by western blotting with C15 antibody. (D) Phosphatase treatment of endogenous GAR22β. GAR22 protein was immunoprecipitated with C15 antibody from serum-starved (48 hours) CAD or COS7 cells and treated with either the serine/threonine phosphatase PP1 or the tyrosine phosphatase TCP. The reactions were run on an SDS-PAGE gel, transferred onto Immobilon membrane and probed with C15 antibody. A mobility shift was observed only in the samples treated with PP1.

proteins can physically crosslink MFs and MTs. To explore this possibility, we transfected pFLAG-hGAR22β and pFLAG-hGAR17β into COS7 cells and stained the cells with a polyclonal anti-tubulin antibody, a monoclonal anti-FLAG antibody, and fluorescently labeled phalloidin. Fluorescently labeled secondary antibodies were used to visualize the FLAG and tubulin stainings. Pictures of the cells were taken at wavelengths suitable for all three labels and superimposed to produce an RGB image. In such an image, areas of triple-color overlay, which would correspond to triple colocalization and probable crosslinking, are represented in white. Significantly more cells transfected with pFLAG-hGAR22β (Fig. 10) exhibited triple colocalization than did cells transfected with pFLAG-hGAR22α, the hGAR22 isoform that does not interact with MTs either in vitro or in vivo. Similar results were obtained with pFLAG-hGAR17β and pFLAG-hGAR17α (data not shown). To quantify the levels of triple colocalization elicited by the pFLAG-hGAR17 or pFLAG-hGAR22 constructs, 30 cells transfected with each construct were selected randomly and their pictures taken. A cell was scored as positive if it contained at least one triple-stained (white) filament equal or exceeding one fifth of the length of the cell or at least two triple-stained filaments each equal or exceeding one tenth of the length of the cell. The χ^2 criterion was used to statistically compare the observed frequencies of triple colocalization (Bailey, 1981). The frequencies of triple colocalization in cells transfected with the β isoforms of both hGAR17 and hGAR22 were found to be significantly (P<0.005) greater than those in cells transfected with their respective α isoforms. These findings indicate that both hGAR22β and hGAR17β are likely to be able to crosslink MFs and MTs in vivo.

We did not observe any differences between the cytoskeleton-binding profiles of hGAR22 and hGAR17 proteins with or

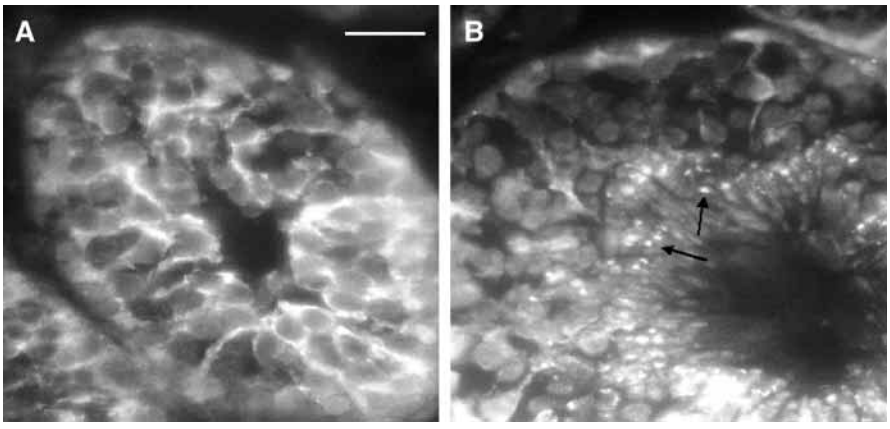

Fig. 9. GAR22 immunohistochemistry of mouse testes. Testicular sections of (A) 3-week- or (B) 5-month old mice were stained with the C15 antibody and TRITC-labeled goat-anti-rabbit secondary antibody. The staining is localized predominantly in the cytoplasm of the germ cells and in the heads of the spermatozoa (indicated with arrows). The staining is likely to represent mGAR22β since it is the only protein recognized by C15 antibody on western blots of mouse testes. Bar, 20 μm.

without a FLAG epitope tag (data not shown). It is therefore highly unlikely that the proposed crosslinking ability of the β isoforms results from the presence of a FLAG tag at their N-terminus.

Discussion

We have characterized the protein products of the *hGAR22* gene and found that they can bind both MFs and MTs in vitro and in vivo. We have also cloned the cDNAs of *mGAR22* and *hGAR17*, another human *Gas2*-like gene. Human and mouse GAR22 proteins are extremely well conserved. In turn, the hGAR17 isoforms are remarkably similar to the hGAR22 proteins both in sequence and in cytoskeleton-binding properties. The longer protein isoforms of the two genes, hGAR22β and hGAR17β, appear to be capable of crosslinking MFs and MTs in vivo.

Both hGAR22α and hGAR22β contain a functional ABD of the CH family and associate with actin filaments in transfected cells. They also bind MFs in spin-down binding assays, indicating that the association with actin filaments observed in vivo is likely to be direct. This association is mediated by the CH domain, which is present in both isoforms. Both hGAR22α and hGAR22β also contain the previously characterized MTBD of the GAR family (Sun et al., 2001). The GAR domain of hGAR22α appears to be masked, since this isoform does not associate with MTs either in transfected cells or in vitro. By contrast, the longer hGAR22β protein associates with MTs in transfected cells as well as in spin-down assays. hGAR22β contains a second MT-binding motif in its C-terminal tail. Various protein structure prediction programs failed to identify any known types of domains or motifs in this portion of hGAR22β (amino acids 338-681), and this region is predicted to be mostly unstructured. Our preliminary data indicate that the sequence responsible for the MT-binding capacity of this region is located between amino acids 338 and 489. Although both the GAR domain and the C-terminal tail of hGAR22β associate with MTs, the GAR domain binds more efficiently than C-terminal tail (especially in vivo). A protein combining the GAR domain and the C-terminal tail not only binds MTs but also appears to bundle them in the majority of transfected cells. Furthermore, this protein also stabilizes MTs and protects them from depolymerization by nocodazole. These findings indicate that the GAR domain and the C-tail may bind MTs cooperatively, resulting in a higher avidity of

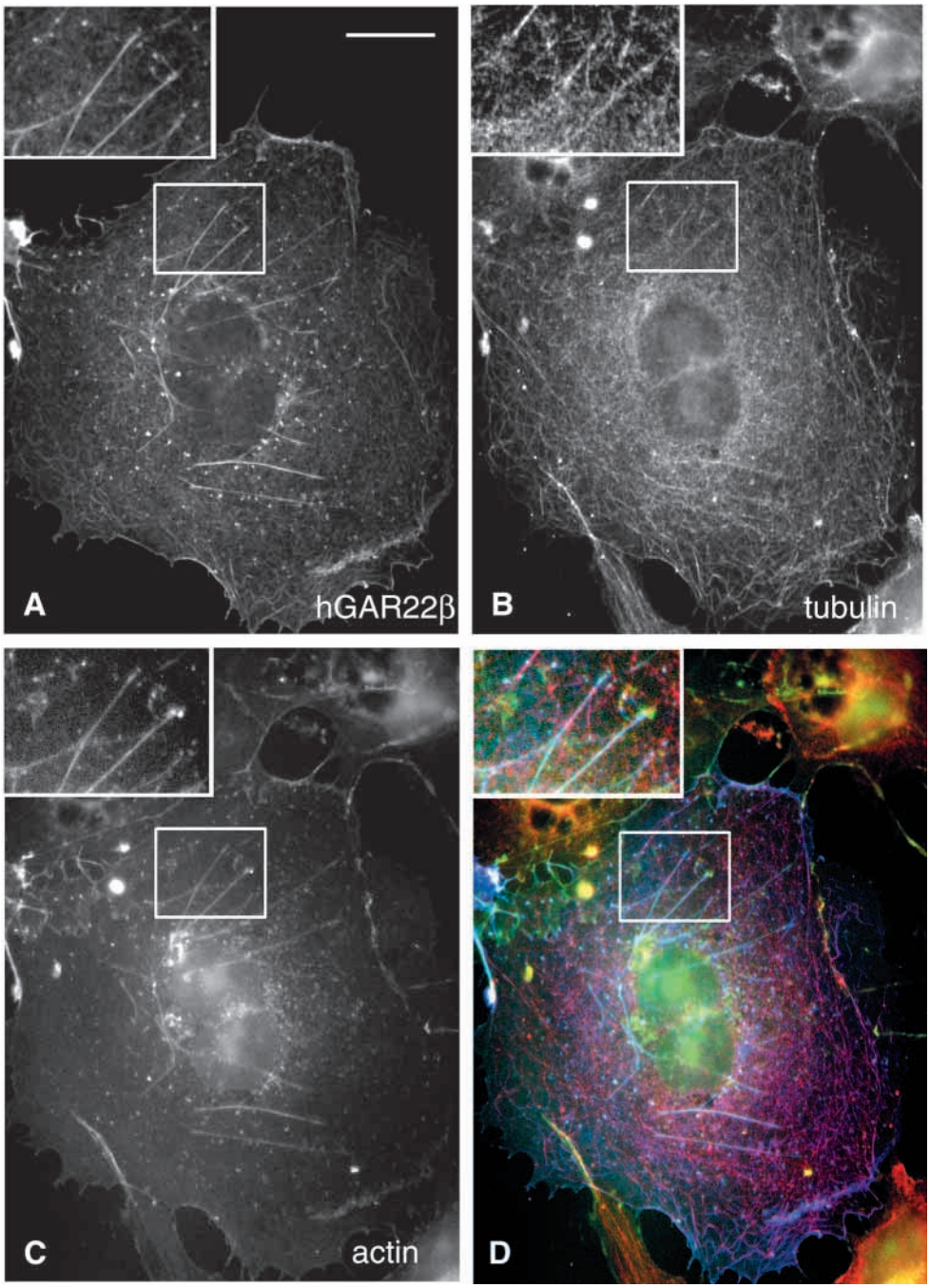

Fig. 10. hGAR22β bridges MFs and MTs in transfected cells. COS7 cells were transiently transfected with pFLAG-hGAR22β and triple stained with a monoclonal anti-FLAG antibody (A), a polyclonal anti-tubulin antibody (B) and phalloidin-AlexaFluor-350 (C). (D) A superimposed image, with the FLAG staining in blue, the tubulin staining in red and the actin staining in green. Triple-stained filaments, probably resulting from crosslinking by hGAR22β, are white colored. Bar, 10 μm.

interaction. This enhanced MT-binding capacity appears to be negated by the presence of the N-terminal CH domain in the full-length isoform. Protease cleavage of hGAR22β under specific physiological circumstances could potentially release a GAR-domain-containing C-terminal fragment that would be able to stabilize MTs. However, we have found no evidence for such a cleavage (see below). Using a combined RACE and RT-PCR approach, we have also cloned two cDNA species of *mGAR22*. The mGAR22 transcripts encode proteins that are extremely similar to hGAR22α and hGAR22β (89% and 86% amino acid identity for the α and β isoforms, respectively). In transfected cells, the cytoskeleton-binding properties of mGAR22α and mGAR22β appear to be identical to those of their human counterparts.

A database search indicated that human chromosome 17 contains a *GAR22*-like gene. We cloned two hGAR17 cDNA species by nested PCR using a human multiple-tissue cDNA library as the template. These cDNAs encode two protein isoforms, hGAR17α and hGAR17β, that share significant sequence similarity with the hGAR22 proteins. The smaller hGAR17 isoform, hGAR17α, contains a CH domain and binds MFs in vitro and in vivo. Its characteristics are generally analogous to those of hGAR22α. The larger hGAR17 isoform, hGAR17β, contains both a CH domain and a GAR domain. These domains are functional, as hGAR17β colocalizes with MFs and MTs in transfected cells and cosediments with both types of filaments in spin-down assays. The overall structure and properties of hGAR17β are similar to those of hGAR22β. Northern blot analysis indicates that hGAR17 mRNA is expressed selectively in skeletal muscle. We do not yet have any information regarding the hGAR17 protein expression pattern.

A number of proteins have been identified that can crosslink different components of the cytoskeleton. Many of these proteins belong to the plakin protein family (Svitkina et al., 1996; Wiche, 1998; Leung et al., 2002); some of them have been shown to simultaneously interact with MFs and MTs in transfected cells. Our laboratory has previously demonstrated that two members of the plakin family, microtubule actin crosslinking factor, MACF, and BPAG1a, can bridge MFs and MTs (Leung et al., 1999a; Leung et al., 2001). Certain non-plakin cytoskeleton-associated proteins, such as MAP1 and MAP2, can do so in vitro (Pedrotti et al., 1994; Pedrotti and Islam, 1997; Ozer and Halpain, 2000). We have found that the larger isoforms of hGAR22 and hGAR17, hGAR22β and hGAR17β, increase the extent of coalignment of MFs and MTs in transfected COS7 cells, most probably by crosslinking the two types of filaments. Thus, the physiological functions of these proteins may involve mediation of specific MF-MT interactions.

Gas2 protein is induced in cultured cells upon growth arrest (Brancolini et al., 1992). It has also been implicated in the apoptosis-associated rearrangement of the cytoskeleton both in cultured cells (Brancolini et al., 1995) and possibly in developing mammalian tissues (Lee et al., 1999). Caspase 3 is the main enzyme responsible for Gas2 cleavage in apoptotic cells (Sgorbissa et al., 1999), and the N-terminal CH-domain-containing product of the cleavage affects the changes in the cytoskeleton observed in cells undergoing apoptosis. We were unable to detect hGAR22 protein cleavage in a variety of cell lines treated with several apoptotic stimuli (data not shown). The expression of either full-length hGAR22 isoforms or the CH domain-containing N-terminus in transfected COS7 cells does not result in any notable changes in cell morphology. Although hGAR22 protein expression is also induced by growth arrest in cultured cells, the absolute levels of expression appear to be low. Thus, we have been unable to visualize endogenous GAR22 protein in several types of arrested cells by indirect immunofluorescent staining with a number of anti-GAR22 antibodies (data not shown). The levels of expression in mouse testis and brain, the only tissues with detectable amounts of endogenous GAR22 protein, are also low. Notably, it is only the larger GAR22β isoform that can be detected in both cultured cells and mouse tissues. Consistent with the GAR22β transcript being the predominant splice-form in both human and mouse tissues, GAR22α protein is undetectable in mouse tissues as well as in cultured cells. Gas2 protein is phosphorylated on serine and threonine during the G0 to G1 transition, which is thought to be a mechanism of rapid Gas2 inactivation following serum stimulation of arrested cells (Brancolini and Schneider, 1994). By contrast, we have found that endogenous GAR22β is heavily phosphorylated on serine and/or threonine in quiescent, G0-arrested cells. Most of the phosphorylation probably occurs on the C-tail sequence, which contains multiple putative PKA, PKC and casein kinase II target sites. On the basis of the differences between Gas2 and GAR22 mentioned above, we believe that the in vivo function of GAR22 is different from that of Gas2. Further studies will be required to determine the physiological roles of GAR22 and GAR17 proteins.

References

Bailey, N. T. J. (1981). *Statistical Methods in Biology*. New York: Halsted Press.

Brancolini, C., Bottega, S. and Schneider, C. (1992). Gas2, a growth arrest-specific protein, is a component of the microfilament network system. *J. Cell Biol.* **117**, 1251-1261.

Brancolini, C. and Schneider, C. (1994). Phosphorylation of the growth arrest-specific protein Gas2 is coupled to actin rearrangements during $G_0 \rightarrow G_1$ transition in NIH 3T3 cells. *J. Cell Biol.* **124**, 743-756.

Brancolini, C., Benedetti, M. and Schneider, C. (1995). Microfilament reorganization during apoptosis: the role of Gas2, a possible substrate for ICE-like proteases. *EMBO J.* **14**, 5179-5190.

Herrmann, H. and Aebi, U. (2000). Intermediate filaments and their associates: multi-talented structural elements specifying cytoarchitecture and cytodynamics. *Curr. Opin. Cell Biol.* **12**, 79-90.

Lee, K. K., Tang, M. K., Yew, D. T., Chow, P. H., Yee, S. P., Schneider, C. and Brancolini, C. (1999). gas2 is a multifunctional gene involved in the regulation of apoptosis and chondrogenesis in the developing mouse limb. *Dev. Biol.* **207**, 14-25.

Leung, C. L., Sun, D., Zheng, M., Knowles, D. R. and Liem, R. K. H. (1999a). Microtubule actin cross-linking factor (MACF): a hybrid of dystonin and dystrophin that can interact with the actin and microtubule cytoskeletons. *J. Cell Biol.* **147**, 1275-1285.

Leung, C. L., Sun, D. and Liem, R. K. (1999b). The intermediate filament protein peripherin is the specific interaction partner of mouse BPAG1-n (dystonin) in neurons. *J. Cell Biol.* **144**, 435-446.

Leung, C. L., Zheng, M., Prater, S. M. and Liem, R. K. (2001). The BPAG1 locus: alternative splicing produces multiple isoforms with distinct cytoskeletal linker domains, including predominant isoforms in neurons and muscles. *J. Cell Biol.* **154**, 691-698.

Leung, C. L., Green, K. J. and Liem, R. K. (2002). Plakins: a family of versatile cytolinker proteins. *Trends Cell Biol.* **12**, 37-45.

Ozer, R. S., and Halpain, S. (2000). Phosphorylation-dependent localization of microtubule-associated protein MAP2c to the actin cytoskeleton. *Mol. Biol. Cell* **11**, 3573-3587.

Pedrotti, B., Colombo, R. and Islam, K. (1994). Microtubule associated protein MAP1A is an actin-binding and crosslinking protein. *Cell Motil. Cytoskeleton* **29**, 110-116.

Pedrotti, B. and Islam, K. (1997). Estramustine phosphate but not estramustine inhibits the interaction of microtubule associated protein 2 (MAP2) with actin filaments. *FEBS Lett.* **403**, 123-126.

Qi, Y., Wang, J. K., McMillian, M. and Chikaraishi, D. M. (1997). Characterization of a CNS cell line, CAD, in which morphological differentiation is initiated by serum deprivation. *J. Neurosci.* **17**, 1217-1225.

Schaerer-Brodbeck, C. and Riezman, H. (2000). Interdependence of filamentous actin and microtubules for asymmetric cell division. *Biol. Chem.* **381**, 815-825.

Schneider, C., King, R. M. and Philipson, L. (1988). Genes specifically expressed at growth arrest of mammalian cells. *Cell* **54**, 787-793.

Sgorbissa, A., Benetti, R., Marzinotto, S., Schneider, C. and Brancolini, C. (1999). Caspase-3 and caspase-7 but not caspase-6 cleave Gas2 in vitro: implications for microfilament reorganization during apoptosis. *J. Cell Sci.* **112**, 4475-4482.

Svitkina, T. M., Verkhovsky, A. B. and Borisy, G. G. (1996). Plectin sidearms mediate interaction of intermediate filaments with microtubules and other components of the cytoskeleton. *J. Cell Biol.* **135**, 991-1007.

Sun, D., Leung, C. L. and Liem, R. K. (2001). Characterization of the microtubule-binding domain of microtubule actin cross-linking factor (MACF): identification of a novel group of microtubule-associated proteins. *J. Cell Sci.* **114**, 161-172.

Tascou, S., Nayernia, K., Samani, A., Schmidtke, J., Vogel, T., Engel, W. and Burfeind, P. (2000). Immortalization of murine male germ cells at a discrete stage of differentiation by a novel directed promoter-based selection strategy. *Biol. Reprod.* **63**, 1555-1561.

Wiche, G. (1998). Role of plectin in cytoskeleton organization and dynamics. *J. Cell Sci.* **111**, 2477-2486.

Yang, Y., Dowling, J., Yu, Q. C., Kouklis, P., Cleveland, D. W. and Fuchs, E. (1996). An essential cytoskeletal linker protein connecting actin microfilaments to intermediate filaments. *Cell* **86**, 655-665.

Yang, Y., Bauer, C., Strasser, G., Wollman, R., Julien, J.-P. and Fuchs, E. (1999). Integrators of the cytoskeleton that stabilize microtubules. *Cell* **98**, 229-238.

Zucman-Rossi, J., Legoix, P. and Thomas, G. (1996). Identification of new members of the Gas2 and Ras families in the 22q12 chromosome region. *Genomics.* **38**, 247-254.